**Cell Reports, Volume *23***

## Supplemental Information

# Induction and Maintenance of CX3CR1-Intermediate Peripheral Memory CD8$^+$ T Cells by Persistent Viruses and Vaccines

**Claire Louse Gordon, Lian Ni Lee, Leo Swadling, Claire Hutchings, Madeleine Zinser, Andrew John Highton, Stefania Capone, Antonella Folgori, Eleanor Barnes, and Paul Klenerman**

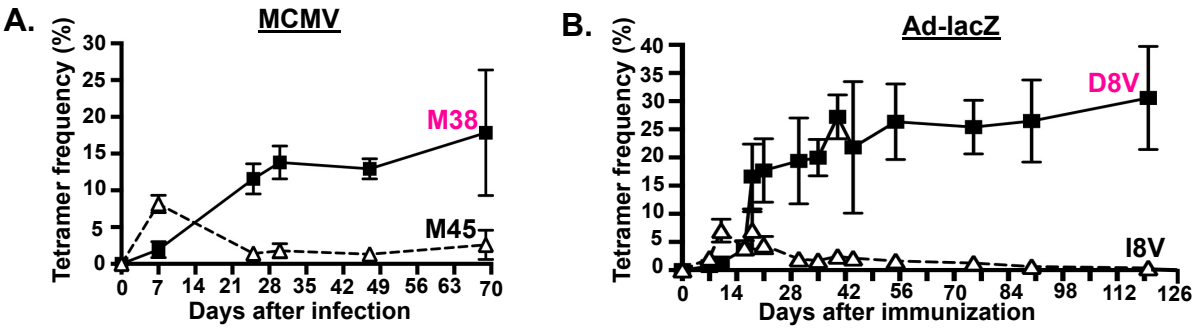
A.
MCMV
Tetramer frequency (%)
30
25
20
15
10
5
0
M38
M45
0 7 14 21 28 35 42 49 56 63 70
Days after infection
B.
Ad-lacZ
Tetramer frequency (%)
40
35
30
25
20
15
10
5
0
D8V
I8V
0 14 28 42 56 70 84 98 112 126
Days after immunization

**Figure S1: MCMV infection and Ad-lacZ immunization induces conventional and inflating CD8$^+$ T cell memory responses, related to Figures 1 and 2**

*Cx3cr1*$^{+/gfp+}$ mice were infected intravenously (iv) with $10^6$ pfus MCMV or $2x10^9$ pfu Ad-lacZ and blood was serially sampled post-immunization (dpi). Conventional memory responses (black label) were assessed by M45 (MCMV)- and I8V(Ad-lacZ)- tetramer staining, and inflationary memory responses (pink label) were assessed M38(MCMV)- and D8V(Ad-lacZ)- tetramer staining (coloring is consistent for all Supplemental Figures). (A) Compiled results showing mean (±SD) tetramer frequency of M45- (open triangle, dotted line) and M38- (filled square, solid line)-tetramer$^+$ CD8$^+$ T cells (n=2-4). (B) Compiled results showing mean (±SD) I8V- (open triangle, dotted line) and D8V- (filled square, solid line) tetramer$^+$ CD8$^+$ T cells (n=3-19).

Figure S2

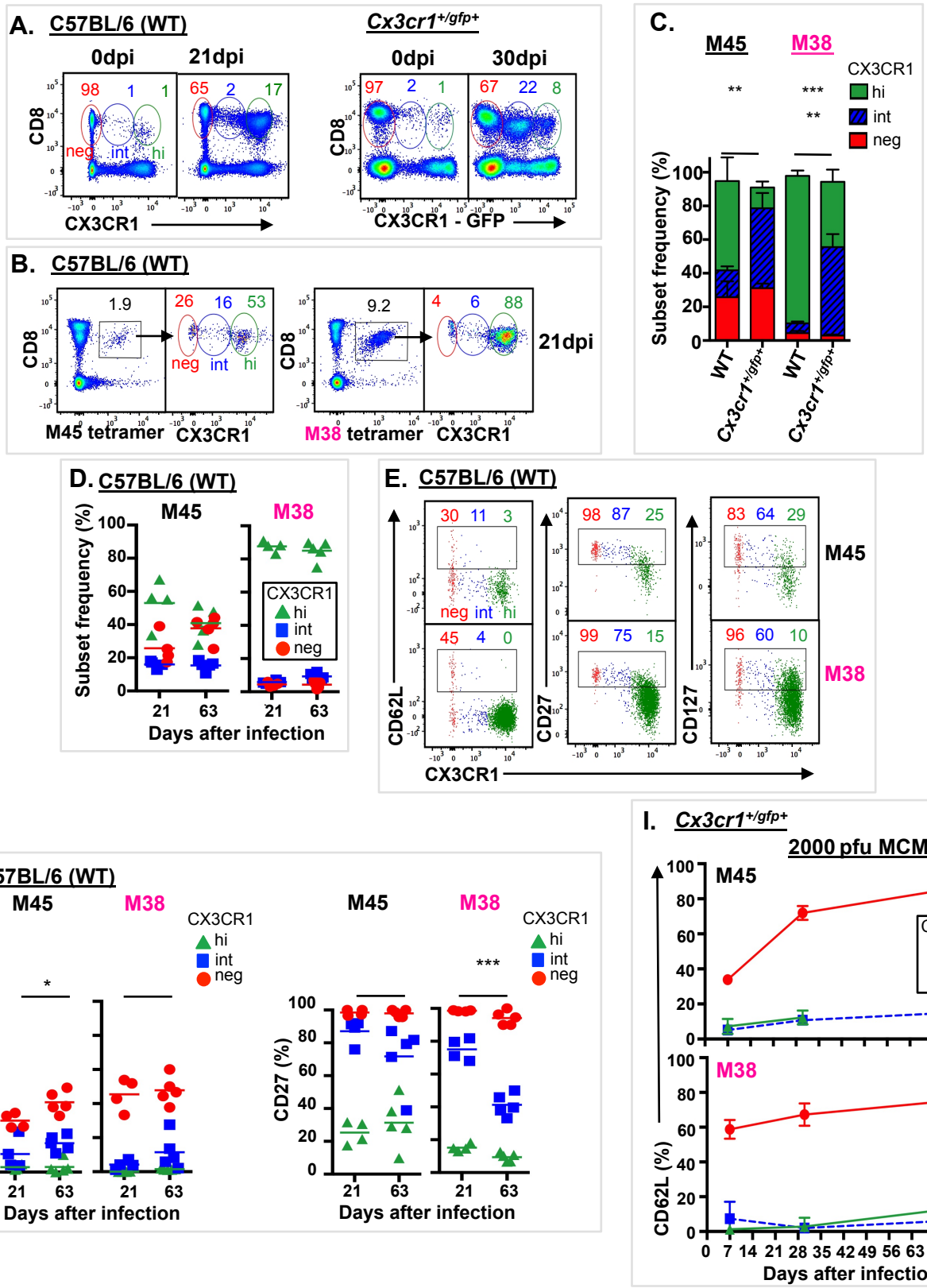
A. C57BL/6 (WT)
Cx3cr1+/gfp+
0dpi
21dpi
30dpi
CD8
CX3CR1
CX3CR1 - GFP
neg
int
hi
B. C57BL/6 (WT)
21dpi
M45 tetramer CX3CR1
M38 tetramer CX3CR1
C.
M45
M38
CX3CR1
hi
int
neg
Subset frequency (%)
WT
Cx3cr1+/gfp+
D. C57BL/6 (WT)
Days after infection
E. C57BL/6 (WT)
CD62L
CD27
CD127
F. C57BL/6 (WT)
CD62L (%)
CD27 (%)
I. Cx3cr1+/gfp+
2000 pfu MCMV
Days after infection
G. C57BL/6 (WT)
83-330dpi
SPL LUNG
10⁶ pfu MCMV
5x10⁴ pfu
WT2639 MCMV
H. C57BL/6 (WT)
Lung
M45 90dpi
M38 90dpi
CD69-CD103-
CD69+CD103-
CD69-CD103+
CD69+CD103+

**Figure S2: MCMV infection induces three distinct CD8$^+$ T cell populations based on CX3CR1 expression in C57BL/6 and *Cx3cr1*$^{+/gfp+}$ mice, related to Figure 1**

*Cx3cr1*$^{+/gfp+}$ and C57BL/6 (wild type; WT) mice were infected intravenously (iv) with $10^6$ pfu or 2000 pfu MCMV. Conventional memory and inflationary memory responses were assessed by M45- and M38-tetramer staining, respectively. (A) Composite FACS plots of CD8 and CX3CR1 staining of live lymphocytes in blood from C57BL/6 (left panel) or *Cx3cr1*$^{+/gfp+}$ (right panel) mice at 0 days post infection (dpi), 21dpi (C57BL/6) or 30 dpi (*Cx3cr1*$^{+/gfp+}$) with $10^6$ pfu MCMV. Mean percentages of CX3CR1 subsets (negative[neg]=red, intermediate[int]=blue, high[hi]=green) of live CD8$^+$ T cells are indicated (C57BL/6 n=4 mice, *Cx3cr1*$^{+/gfp+}$ n=3 mice). (B) Composite FACS plots of M45- and M38-tetramer staining of live lymphocytes (left) and CX3CR1 subsets of tetramer-specific CD8$^+$ T cells (right) in blood from C57BL/6 mice, 21 dpi with $10^6$ pfu MCMV. Mean live tetramer$^+$ CD8$^+$ T cells and mean CX3CR1 subsets are indicated (n=4). (C) Compiled results comparing mean (±SD) of CX3CR1 subsets (neg=red, int=blue, hi=green) of M45- and M38-tetramer$^+$ CD8$^+$ T cells in blood from C57BL/6 (WT) or *Cx3cr1*$^{+/gfp+}$ mice, 21 or 30 dpi with $10^6$ pfu MCMV, respectively (C57BL/6 n=4 mice, *Cx3cr1*$^{+/gfp+}$ n=3 mice). (D) Individual CX3CR1 subset frequencies and means of M45- and M38-tetramer$^+$ CD8$^+$ T cells in blood from C57BL/6 (WT) mice 21 and 63 dpi (n=4 and n=5, respectively). (E-F) Expression of cell surface markers CD62L, CD27 and CD127 by CX3CR1 subsets in M45- and M38-tetramer$^+$ CD8$^+$ T cells in C57BL/6 mice 21 or 63 dpi with $10^6$ pfu MCMV. (E) Composite FACS plots of CD62L (left panel), CD27 (middle panel) and CD127 (right panel) expression in M45- and M38-tetramer$^+$ CD8$^+$ T cells at 21 dpi. Mean expression of indicated marker for each CX3CR1 subset is shown (n=4). (F) Shown are individual and mean CX3CR1 subset expression of CD62L (left panel) and CD27 (right panel) in M45- and M38-tetramer$^+$ CD8$^+$ T cells in blood from C57BL/6 (WT) mice 21 and 63 dpi (n=4/each and n=5/each, respectively).(G) CX3CR1 subset distribution of M38- and M45- tetramer+ cells was assessed in spleen (SPL), liver (LIV) and lung of C57BL/6 (WT) mice following infection with $10^6$ pfu (solid symbols, 330dpi) or 50000 pfu (open symbols, 83dpi) of WT2639 MCMV (considered to be a full dose). (H) Frequency of co-expression of CD69 and CD103 in M45- and M38-tetramer$^+$ CD8$^+$ T cells in lung from C57BL/6 mice 83dpi (n=3). (I) Compiled results showing mean (±SD) CD62L expression by CX3CR1 subsets in M45- and M38-tetramer$^+$ CD8$^+$ T cells following infection with 2000 pfu MCMV (n=5-9). Significant differences were determined by 1-way ANOVA and corrected for multiple comparisons (Holm-Sidak). P=0.05 to 0.011 (*), p=0.01 to 0. 001 (**) and p<0.001 (***). All FACS plots are composite plots generated by randomly selecting equal numbers of the cell population of interest from each subject.

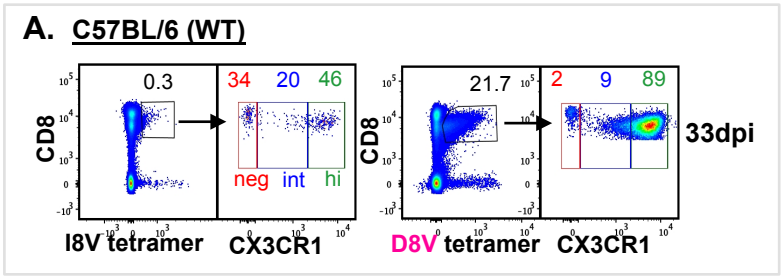
A. C57BL/6 (WT)
0.3
34 20 46
neg int hi
CD8
I8V tetramer
CX3CR1
21.7
2 9 89
D8V tetramer
33dpi

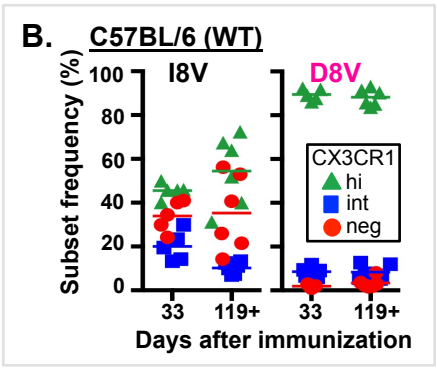
B. C57BL/6 (WT)
I8V
D8V
Subset frequency (%)
CX3CR1
hi
int
neg
33
119+
Days after immunization

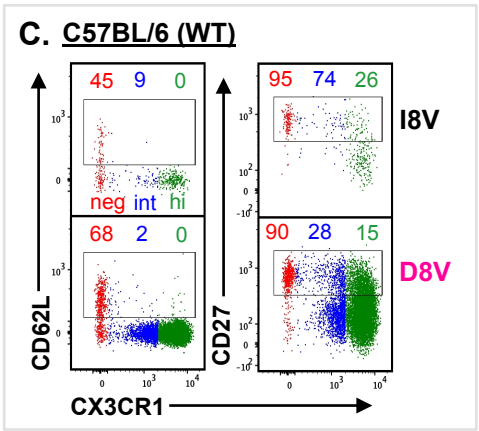
C. C57BL/6 (WT)
45 9 0
neg int hi
68 2 0
95 74 26
90 28 15
I8V
D8V
CD62L
CD27
CX3CR1

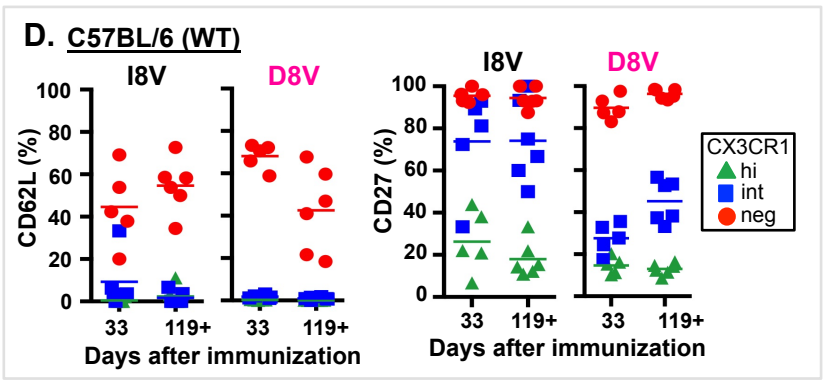
D. C57BL/6 (WT)
I8V
D8V
CD62L (%)
CD27 (%)
CX3CR1
hi
int
neg
33
119+
Days after immunization

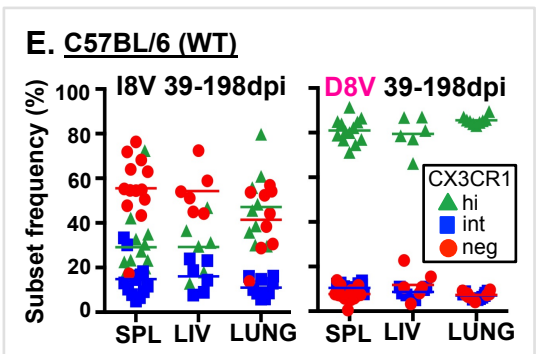
E. C57BL/6 (WT)
I8V 39-198dpi
D8V 39-198dpi
Subset frequency (%)
CX3CR1
hi
int
neg
SPL
LIV
LUNG

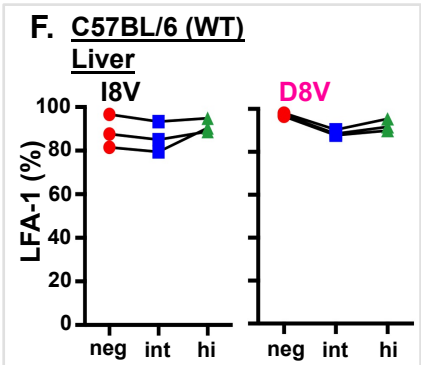
F. C57BL/6 (WT)
Liver
I8V
D8V
LFA-1 (%)
neg
int
hi

**Figure S3: Ad-lacZ immunization induces three distinct CD8$^+$ T cell populations based on CX3CR1 expression in C57BL/6 mice, related to Figure 2**

C57BL/6 (wild type; WT) mice were infected intravenously (iv) with 2x10$^9$ pfu of a recombinant replication-deficient HuAd5 vector expressing lacZ (Ad-lacZ). Conventional memory and inflationary memory responses were assessed by I8V- and D8V-tetramer staining, respectively. (A) Composite FACS plots of I8V- and D8V-tetramer staining of live lymphocytes (left) and CX3CR1 subsets of tetramer-specific CD8$^+$ T cells (right) in blood from C57BL/6 (WT) mice at 33 days post immunization (dpi) with 2x10$^9$ pfu Ad-lacZ. Mean CX3CR1 subsets (negative[neg]=red, intermediate[int]=blue, high[hi]=green) of live CD8$^+$ T cells are indicated (n=4 mice). (B) Shown are individual and mean CX3CR1 subset frequency of I8V- and D8V-tetramer$^+$ CD8$^+$ T cells in blood from C57BL/6 (WT) mice 33 and 119+ dpi (n=5 and n=6, respectively). (C-D) Expression of cell surface markers CD62L and CD27 by CX3CR1 subsets in I8V- and D8V-tetramer$^+$ CD8$^+$ T cells in C57BL/6 mice 33 or 119+ dpi with 2x10$^9$ pfu Ad-lacZ. (C) Shown is representative flow cytometry plots of CD62L (left panel) and CD27 (middle panel) expression in I8V- and D8V-tetramer$^+$ CD8$^+$ T cells at 33 dpi. Mean expression of indicated marker for each CX3CR1 subset is shown (n=5). (D) Individual and mean CX3CR1 subset expression of CD62L (left panel) and CD27 (right panel) in I8V- and D8V-tetramer$^+$ CD8$^+$ T cells in blood from C57BL/6 (WT) mice 33 and 119+ dpi (n=5 and n=6, respectively). (E) Individual and mean CX3CR1 subset frequencies of I8V- and D8V- tetramer+ cells in spleen (SPL), liver (LIV) and lung 39-198dpi (n=6-13). (F) Expression of LFA-1 in I8V- and D8V-tetramer$^+$ CD8$^+$ T cells in liver from C57BL/6 mice 198dpi (n=3). Significant differences were determined by one-way ANOVA and corrected for multiple comparisons (Holm-Sidak). P=0.05 to 0.011 (*), p=0.01 to 0. 001 (**) and p<0.001 (***). All FACS plots are composite plots generated by randomly selecting equal numbers of the cell population of interest from each subject.

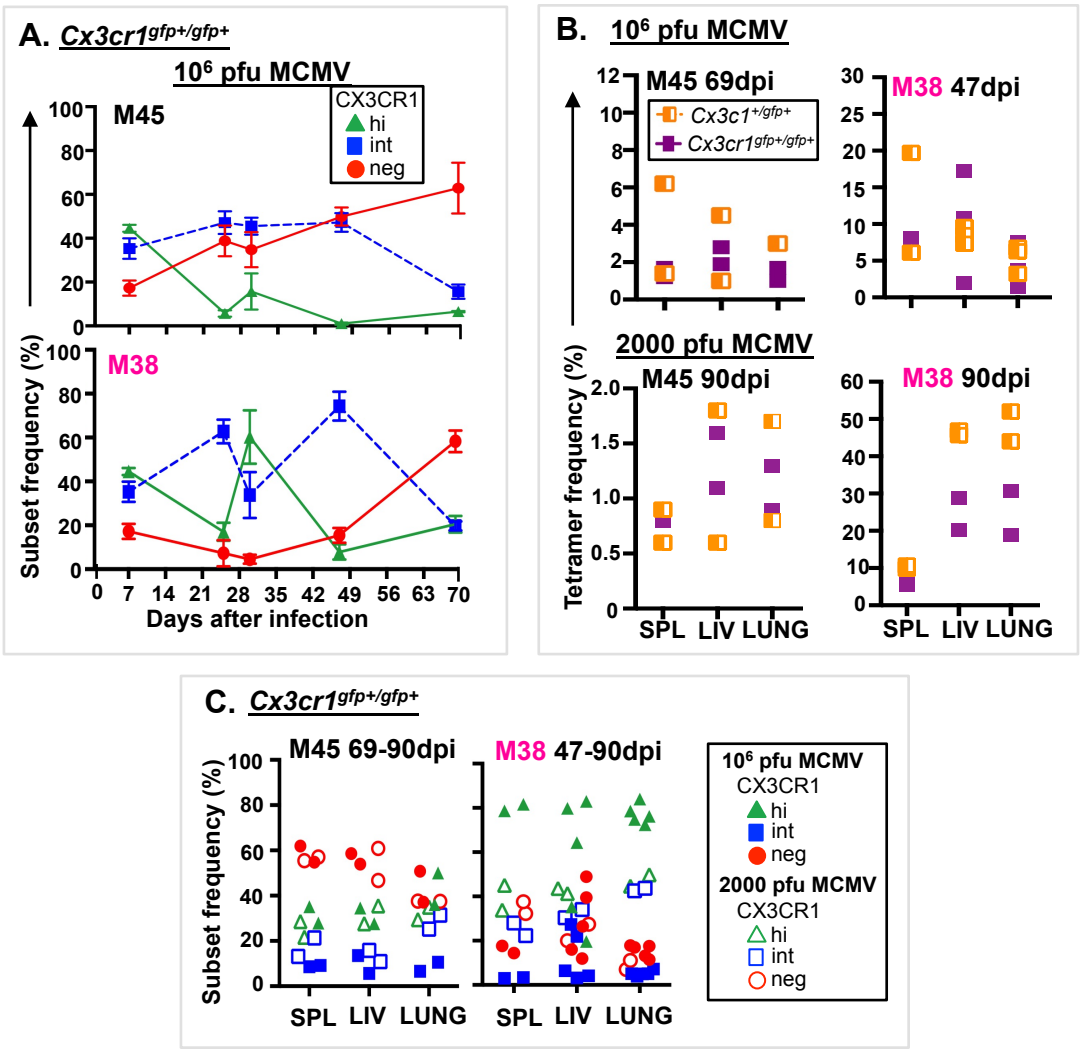
A. Cx3cr1gfp+/gfp+
10⁶ pfu MCMV
M45
M38
CX3CR1
hi
int
neg
Subset frequency (%)
Days after infection
B. 10⁶ pfu MCMV
M45 69dpi
M38 47dpi
Cx3c1+/gfp+
Cx3cr1gfp+/gfp+
2000 pfu MCMV
M45 90dpi
M38 90dpi
Tetramer frequency (%)
SPL LIV LUNG
C. Cx3cr1gfp+/gfp+
M45 69-90dpi
M38 47-90dpi
Subset frequency (%)
SPL LIV LUNG
10⁶ pfu MCMV
CX3CR1
hi
int
neg
2000 pfu MCMV
CX3CR1
hi
int
neg

**Figure S4: CX3CR1 is not required for optimal inflating responses following MCMV infection, related to Figure 4**

*Cx3cr1*$^{gfp+/gfp+}$ and *Cx3cr1*$^{+/gfp}$ mice were infected intravenously (iv) with $10^6$ pfu or 2000 pfu MCMV and blood was serially sampled up to 70 days post-infection (dpi). Memory responses were assessed by M45 and M38 tetramer staining. (A) Compiled results showing mean (±SD) CX3CR1 subsets (neg=red circle, int=blue square, hi=green triangle) of M45- and M38-tetramer$^+$ CD8$^+$ T cells in *Cx3cr1*$^{gfp+/gfp+}$ mice following infection with $10^6$ pfu MCMV (n=2-4 mice/each). (B) Individual tetramer frequencies of M45- and M38-tetramer$^+$ CD8$^+$ T cells in spleen (SPL), liver (LIV) and lung from *Cx3cr1*$^{+/gfp+}$ (orange half filled square, n=2-3 mice/each) and *Cx3cr1*$^{gfp+/gfp+}$ (purple filled square, n=3-4 mice/each) mice 47-90 dpi infection with $10^6$ pfu (top panel) or 2000 pfu (bottom panel) MCMV. (C) Shown are individual CX3CR1 subset frequencies for M45- and M38-tetramer$^+$ CD8$^+$ T cells in indicated tissues, 47-90 dpi with $10^6$ pfu (closed symbol) or 2000 pfu (open symbol) MCMV. Significant were determined by one-way ANOVA and corrected for multiple comparisons (Holm-Sidak). P=0.05 to 0.011 (*), p=0.01 to 0. 001 (**) and p<0.001 (***).

**Figure S5**

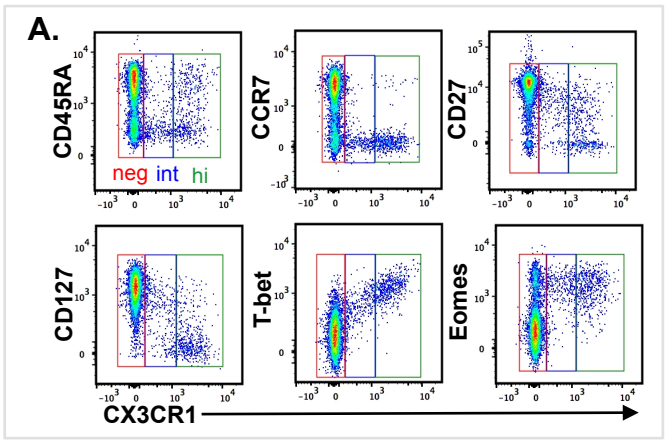
A.
CD45RA
neg int hi
CCR7
CD27
CD127
T-bet
Eomes
CX3CR1

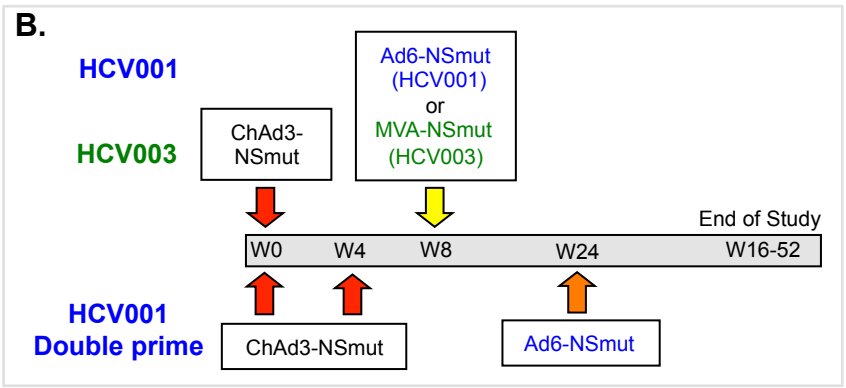
B.
HCV001
HCV003
ChAd3-NSmut
Ad6-NSmut (HCV001) or MVA-NSmut (HCV003)
End of Study
W0
W4
W8
W24
W16-52
HCV001 Double prime
ChAd3-NSmut
Ad6-NSmut

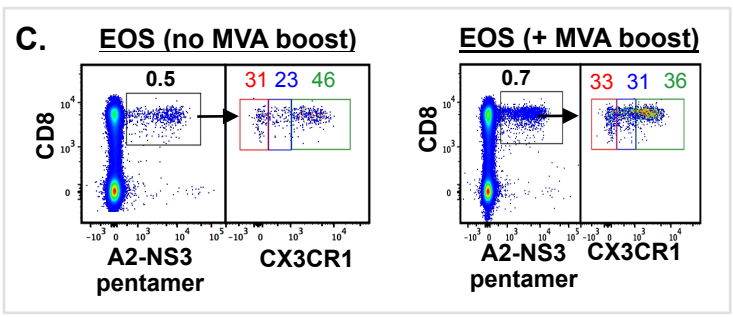
C.
EOS (no MVA boost)
EOS (+ MVA boost)
CD8
0.5
31 23 46
0.7
33 31 36
A2-NS3 pentamer
CX3CR1

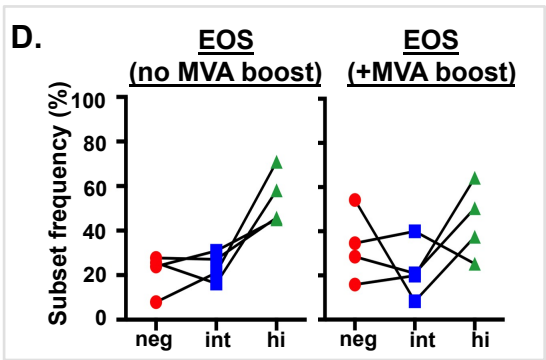
D.
EOS (no MVA boost)
EOS (+MVA boost)
Subset frequency (%)
100
80
60
40
20
0
neg
int
hi

**Figure S5: Phenotype of CX3CR1 subsets on polyclonal and adenoviral vaccine-derived CD8$^+$ T cells, related to Figures 5-6**

(A) Expression of cell surface markers (CD27 and CD127) and transcription factors (T-bet, Eomes) by CX3CR1 subset was assessed in A2-NS3 pentamer-negative CD8$^+$ T cells in blood taken from 5 volunteers. Shown are composite FACS plots (n=5) of CX3CR1 expression and indicated marker, gated on live CD8+ T cells with CX3CR1 subset highlighted (neg=red, int=blue, hi=green). (B) Schematic of vaccination protocol. All volunteers received a priming regimen of a replicative defective simian adenoviral vector (ChAd3, $5x10^8$ - $2.5x10^{10}$ viral particles) encoding the NS3, NS4, NS5A, and NS5B proteins of HCV genotype 1b (ChAd3-NSmut) (Swadling et al., 2014). A subset of 5 volunteers also received a boost with a modified vaccinia Ankara (MVA, $2x10^7$ - $2x10^8$ pfu) vector encoding the same HCV genotype 1b proteins (MVA-NSmut) 8 weeks (W) later (Table S2). (C) Blood samples were taken at end of study (TW16-32, "EOS") from all volunteers. Vaccine-derived CD8$^+$ T cells were assessed by staining with HLA-A2 pentamers containing an NS3 epitope (A2-NS3 pentamer; see Table S3 for pentamer details). Shown is composite FACS plots of A2-NS3 pentamer staining (left) of live CD3$^+$ lymphocytes, and CX3CR1 subsets of A2-NS3 pentamer$^+$ CD8$^+$ T cells at EOS in volunteers who did not receive the MVA boost (left, n=4) and those who did (right, n=5). Mean A2-NS3 pentamer$^+$ CD8$^+$ T cell frequency and mean CX3CR1 subset frequency is indicated. (D) Individual CX3CR1 subset frequency of A2-NS3 pentamer$^+$ CD8$^+$ T cells at EOS in volunteers who did not receive the MVA boost (left, n=4) and those who did (right, n=5).

**Table S1: Number of $CD8^+$ T cells isolated from tissues of *Cx3cr1*$^{+/gfp+}$ *and* *Cx3cr1*$^{gfp+/gfp+}$ mice, related to Figure 4**

| | Mean number of $CD8^+$ T cells (no. of mice) | | |
|---|---|---|---|
| **Tissue** | ***Cx3cr1***$^{+/gfp+}$ | ***Cx3cr1***$^{gfp+/gfp+}$ | **P value** |
| *MCMV* | | | |
| Spleen | $2.7x10^8$ (3) | $3.3x10^8$ (4) | 0.59 |
| Liver | $2.6x10^7$(3) | $7.6x10^6$ (4) | 0.06 |
| Lung | $1.7x10^7$ (3) | $2.9x10^7$ (4) | 0.33 |
| *Ad-lacZ* | | | |
| Spleen | $2.3x10^7$ (3) | $8.9x10^6$ (5) | 0.13 |
| Liver | $1.6x10^6$ (4) | $9.9x10^5$ (5) | 0.12 |
| Lung | $1.4x10^6$ (4) | $9.1x10^5$ (5) | 0.36 |

**Table S2: Characteristics of 13 volunteers used for this study, related to Figures 5-7 and Figure S5**

| Volunteer# | Age | Sex | CMV IgG | ChAd3 prime | MVA boost | HCV pentamer[a] | CMV tetramer[a] |
|---|---|---|---|---|---|---|---|
| **006** | 29 | M | - | + | - | A2-NS3 | NA |
| **038** | 25 | F | + | + | - | A2-NS3 | NA |
| **060** | 24 | F | - | + | - | A2-NS3 | NA |
| **068** | 27 | F | - | + | - | A2-NS3 | NA |
| **332** | 21 | M | - | + | + | A2-NS3 | NA |
| **339** | 37 | F | + | + | + | A2-NS3 | A2-pp65 |
| **343** | 31 | M | - | + | + | A2-NS3 | NA |
| **345** | 21 | F | + | + | + | A2-NS3 | A2-pp65 |
| **347** | 26 | M | + | + | + | A2-NS3 | NA |
| **039** | 44 | M | + | NA | NA | NA | A2-pp65 |
| **400** | 28 | M | + | NA | NA | NA | B7-pp65 |
| **401** | 30 | F | + | NA | NA | NA | A2-pp65, A1-pp50 |
| **403** | 54 | M | + | NA | NA | NA | A2-pp65 |

[a]See Table S3 for tetramer and pentamer details
Abbreviations: Male (M), female (F), not applicable (NA), positive (+), negative (-), hepatitis C virus (HCV),

**Table S3: List of vaccine pentamers and CMV tetramers used for studies antigen-specific CD8$^+$ T cells, related to Experimental Procedures**

| HLA type | Target-epitope | Amino acid sequence | Abbreviation | Source |
|---|---|---|---|---|
| *Human* | | | | |
| A*0101 | CMV-pp50 $_{245–253}$ | VTEHDTLLY | A1-pp65 | NIH Tetramer Facility[a] |
| A*0201 | CMV-pp65 $_{495–503}$ | NLVPMVATV | A2-pp65 | NIH Tetramer Facility[a], Proimmune |
| B*0702 | CMV-pp65 $_{417–426}$ | TPRVTGGGAM | B7-pp65 | NIH Tetramer Facility[a] |
| A*0201 | HCV-NS3$_{1406-1415}$ | KLSGLGINAV | A2-NS3 | Proimmune |
| *Mouse* | | | | |
| H-2Db | MCMV-M45$_{985-993}$ | HGIRNASFI | M45 | NIH Tetramer Facility[a] |
| H-2Kb | MCMV-M38$_{316-324}$ | SSPPMFRV | M38 | NIH Tetramer Facility[a] |
| H-2Kb | bgal$_{497-504}$ | ICPMYARV | I8V | NIH Tetramer Facility |
| H-2Kb | bgal$_{96-103}$ | DAPIYTNV | D8V | NIH Tetramer Facility[a] |

[a]Peptide for monomer construction was obtained from Proimmune.

**Table S4: Fluorochrome-conjugated antibodies used in flow cytometry, related to Experimental Procedures**

| Antibody | Fluorochrome | Clone | Manufacturer[a] |
|---|---|---|---|
| *Human* | | | |
| CD3 | PO | UCHT1 | Life Technologies |
| CD8 | AF700 | SK1 | BioLegend |
| CCR7 | PerCp-Cy5.5 | G04H37 | BioLegend |
| CD45RA | FITC | HI100 | Beckton Dickinson |
| CX3CR1 | BV421 | 2A9-1 | BioLegend |
| CD27 | PE-Cy7 | LG.3A10 | BioLegend |
| CD127 | PE/Dazzle594 | A019D5 | BioLegend |
| T-bet | BV605 | 4B10 | BioLegend |
| Eomes | eF660 | WD1928 | eBioscience |
| Viability | LIVE/DEAD near IR | NA | Life Technologies |
| *Mouse* | | | |
| CD8 | eF450 | 53-6.7 | eBioscience |
| CX3CR1 | BV421 | SA011F11 | BioLegend |
| CD62L | AF700 | MEL-14 | BioLegend |
| CD27 | FITC | LG.7F9 | eBioscience |
| CD27 | PerCp-Cy5.5 | LG3A.10 | BioLegend |
| CD127 | PE-Cy7 | A7R34 | eBioscience |
| Thy1.2 | AF700 | 53-2.1 | Biolegend |
| Viability | LIVE/DEAD near IR | NA | Life Technologies |

[a] Antibodies were obtained from BD Biosciences (Oxford, UK), eBioscience (Loughborough, UK), BioLegend (London, UK) and Life Technologies (Loughborough, UK.

Abbreviations: Pacific orange (PO), alexa Fluor (AF), allophycocyanin (APC), brilliant violet (BV), eFluor (eF), infrared (IR), peridinin-chlorophyll-protein (PerCP), phychoerythrin (PE) and fluorescein isothiocyanate (FITC).

Italics denote the species specificity of the antibody